PCCP

Accepted Manuscript

ROYAL SOCIETY OF CHEMISTRY

www.rsc.org/pccp

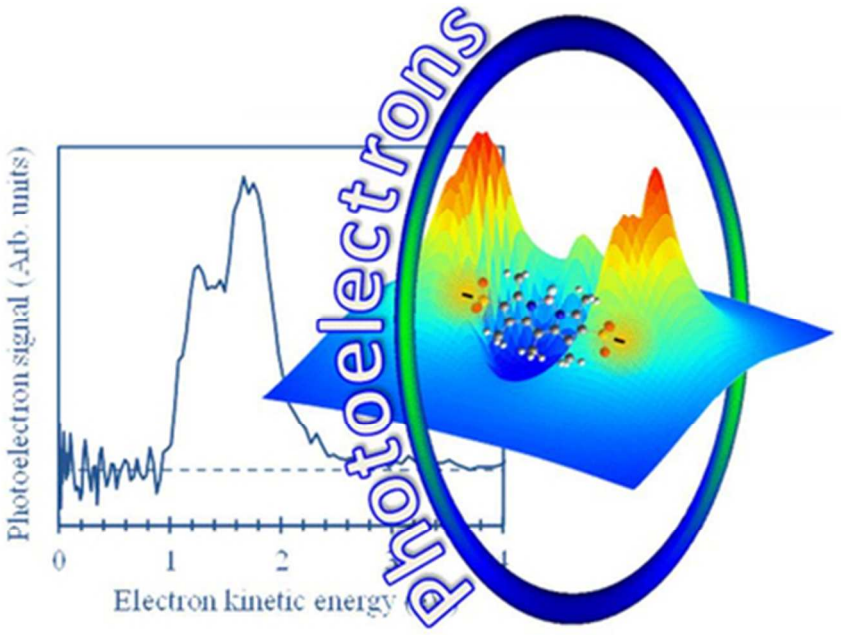

39x26mm (300 x 300 DPI)

Recent progress towards understanding the repulsive Coulomb barrier in multiply-charged anion using photoelectron spectroscopy is discussed.

Cite this: DOI: 10.1039/c0xx00000x

www.rsc.org/xxxxxx

PERSPECTIVE

Excited states of multiply-charged anions probed by photoelectron imaging: Riding the repulsive Coulomb barrier

Jan R. R. Verlet*[a], Daniel A. Horke[b], and Adam S. Chatterley[c]

Received (in XXX, XXX) Xth XXXXXXXXX 20XX, Accepted Xth XXXXXXXXX 20XX

DOI: 10.1039/b000000x

Many properties of isolated multiply-charged anions (MCAs) are dictated by the strong intra-molecular Coulomb interactions that are present. The most striking property of MCAs is a long-range repulsive Coulomb barrier (RCB) that arises from the repulsive interaction between an electron and an anion which must be overcome to form a MCA. Excited states provide a route to probing this RCB and the focus of this Perspective is on recent photoelectron experiments, including angularly and temporally resolved, that have provided detailed physical insight into the RCB surfaces, their anisotropy, and their use to monitor molecular dynamics in real-time. An outlook provides some future prospects that studies on MCAs provide in terms of monitoring structural, charge-migration, and solvation dynamics.

Introduction

The notion that molecular ions can carry more than a single negative charge is not surprising to even a novice chemist, with ubiquitous examples such as SO_4^{2-} and PO_4^{3-}. Their stability is, however, derived from strong interactions with the surroundings. In isolation, both SO_4^{2-} and PO_4^{3-} are thermodynamically unstable with respect to electron loss because of the close proximity of the excess charges.[1] For example, SO_4 has an electron affinity of 5.1 eV,[2] while that of SO_4^- is estimated to be –2.0 eV.[3-6] Thermodynamic instability with respect to dissociation (Coulomb explosion) is similarly affected by the charge proximity in highly-charged negative ions. Yet, despite this strong intramolecular repulsion, dianions, trianions and higher order polyanions or multiply-charged anions (MCAs) (also commonly referred to as multianions) can be stable in the gas-phase. Not only does this important class of ions present a large array of building blocks for chemistry,[7, 8] the close proximity of negative charges makes their physical properties and electronic structure unique and the chemical physics of MCAs has attracted significant interest both theoretically and experimentally.

The stability of MCAs comes from a delicate balance between short-range attraction and the long-range Coulomb repulsion. If one considers an extended linear aliphatic chain with two terminal negatively charged groups, then it is reasonable to assume that, as the chain length tends to infinity, the two charged groups will simply appear as independent anionic groups. However, as the chain length is reduced, the Coulomb repulsion will take hold and will destabilise each negatively charged site. At some inter-charge distance, this repulsion will dominate and the system will be metastable. In this case, for a MCA A^{n-}, the energy of $A^{(n-1)-} + e^-$ will be lower than that of A^{n-}.

When viewed from the $A^{(n-1)-} + e^-$ asymptote, there is a long-range Coulomb interaction that scales as $1/r$, where r is the distance between $A^{(n-1)-}$ and e^-. The net result is that there exists a repulsive interaction that may extend well beyond the molecular framework of A. This repulsive Coulomb barrier (RCB), schematically shown in Figure 1, is a defining feature of isolated MCAs and has been the subject of several excellent reviews.[7-12] The RCB makes MCAs very different from neutrals or cations in which the long-range potential is always attractive, or anions where in general the interaction is attractive except for some small short-range centrifugal barriers that may exist for $l > 0$ partial waves.[13]

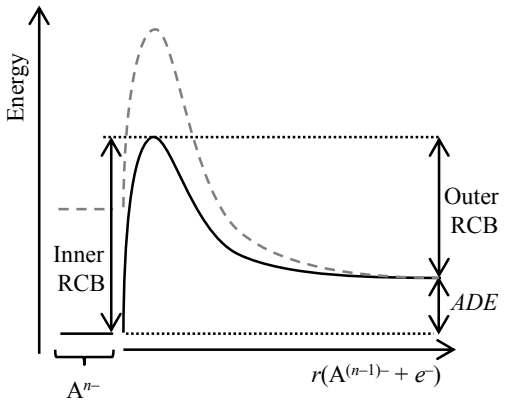

Figure 1: Schematic of the repulsive Coulomb barrier for electron loss from A^{n-} with a positive adiabatic energy (*ADE*) (solid black line) and with a negative *ADE* (dashed grey line).

One of the earliest observations of an isolated dianion was C_{60}^{2-} and other carbon clusters.[14-17] In these, the charges are delocalised and can, on average, be sufficiently separated to overcome the Coulombic repulsion. The experimental study of the RCB was pioneered by the Wang group. They recognised that photoelectron (PE) spectroscopy is highly sensitive to the RCB because the outgoing electron is directly influenced by the

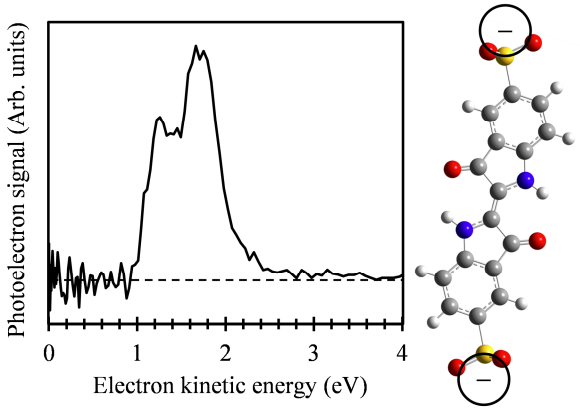

Figure 2: Photoelectron spectrum of the indigo carmine dianion (shown) taken at 4.66 eV, which highlights the presence of the cut-off at *eKE* ~ 1.1 eV, below which no photoelectrons are be emitted. Adapted from Ref. 21, with permission of the PCCP Owner Societies.

barrier.[9, 18-20] In a series of seminal experiments, they showed that the RCB manifests itself in PE spectra as a spectral threshold below which no PEs can be emitted.[18, 19] Irradiation of A^{n-} with photons of energy *hv*, that exceed the adiabatic detachment energy (*ADE*) will lead to PE emission with kinetic energies (*eKE*) in the range:

$$(hv - ADE) \geq eKE \geq \text{RCB} \qquad (1)$$

An example of this is shown in Figure 2 for the indigo carmine dianion in which the excess negative charges are localised on the terminal SO_3^- groups.[21]

The energy of this cut-off is a direct measure of the height of the RCB when viewed from the $A^{(n-1)-} + e^-$ asymptote. This outer RCB is determined by the relative location of the excess negative charges, as shown by the Wang group using PE spectroscopy of the dicarboxylic acids $^-O_2C(CH_2)_mCO_2^-$.[18] Incrementing *m* increases the distance between charge sites (assumed to be localised on the oxygen atoms of the CO_2 groups) with the resultant decrease in RCB height as shown in Figure 3. In a simple electrostatic picture, the RCB height scales as

$$\text{RCB} = \kappa e^2 / 4\pi\varepsilon_0 R, \qquad (2)$$

where *R* is the distance between the two charged sites and $\kappa = 1$. Wang *et al.* found that a scaling of $\kappa = 1.17$ was required to reproduce their estimated RCB height dependence on *R*. Ehrler *et al*. determined $\kappa = 1.58$ for their study on C_{84}^{2-}.[22] The magnitude of κ accounts for polarisability, spatial correlation effects of the electrons and electron delocalisation,[23] which are neglected in a simple electrostatic picture. The larger κ value for C_{84}^{2-} suggests a more delocalised excess electron distribution as might be expected. Figure 3 also shows the increase in the *ADE* as *m* increases. For the cut-off observed in Figure 2, the situation is somewhat different. In this case, the electron emission is from a central chromophore so that the final state is in fact an anion which has two localised terminal negative charges and a positive hole at the centre.[24] The RCB can be estimated in much the same manner by treating each charge as a point charge and calculating the interaction of an e^- with this total potential.[24] This yields an RCB height of 0.84 eV, which corresponds to $\kappa = 1.31$ and this is

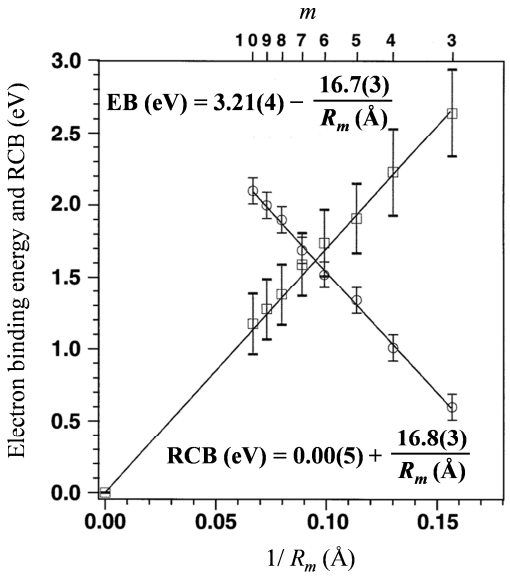

Figure 3: Dependence of the RCB height and electron binding energy as a function of the Coulomb repulsion ($1/R_m$) between the negative charges in $^-O_2C(CH_2)_mCO_2^-$. Adapted from Ref. 18, with permission from American Physical Society.

likely correlated with the delocalised hole. A key point to note is that the height of the RCB effectively provides a distance measurement between well-localised charge sites in a molecular MCA. Hence, PE spectroscopy can be used as an intramolecular ruler.[18] However, it must be noted that, for large MCAs, several conformations can be present (and interconverting), which leads to a smearing out of the cut-off.[25-27]

The RCB can also lead to the formation of metastable MCAs, in which the energy of the ground state of A^{n-} lies between the energy of $A^{(n-1)-} + e^-$ asymptote and the top of the RCB (see Figure 1). In this case, PE spectroscopy leads to PE emission with *eKE* > *hv*. This was first shown for a tetra-sulphonated cyclic copper phthalocyanine tetra-anion and has subsequently been observed in a number of other MCAs.[25, 28-31] As the energy of A^{n-} lies above the $A^{(n-1)-} + e^-$ asymptote, the electron can tunnel through the RCB. If the energy difference between A^{n-} and $A^{(n-1)-}$ is small relative to the RCB, then the lifetimes for electron loss by tunnelling can be sufficiently long (>μs) for the MCA to be isolated by mass-spectrometry.[29] If the lifetime of A^{n-} is shorter, it cannot be observed using mass-spectroscopic methods. However, excited states can be used as sensitive probes of the tunnelling process and dynamics, as discussed below. The observation of electron tunnelling in a well-defined molecular system provides a very elegant route to studying this fundamentally and technologically important process.

A key aspect of the RCB is that it is anisotropic. Returning to the example of an extended linear aliphatic chain with two terminal negatively charged groups, the RCB will peak around the position of the charged groups. Insight into the shape of the RCB can be obtained from electronic structure calculations.[32] In essence, the RCB can be constructed by calculating the difference in total energy between the $A^{(n-1)-} + e^-$ system as a function of the position *r*, and A^{n-}. However, as suggested by Eq. (2), a crude estimate of the RCB can be gained using a simple classical calculation treating an incoming electron as a point charge

interacting with point charges on the $A^{(n-1)-}$ system. This is quite useful as it also allows the overall 3D shape of the surface to be explored. Direct consequences of the anisotropic RCB are that the electron will be emitted primarily from regions where the RCB < $h\nu - ADE$ and that the outgoing electron trajectory is affected by the Coulomb field. As discussed below, the asymptotic distribution of emitted electrons can, in principle, provide detailed insight into the shape of the RCB and hence of the molecular structure of the MCA.

The focus in this Perspective is on the shape and nature of the RCB, its consequences on the photoelectron spectroscopy of MCAs and to highlight some of the key developments that have arisen over the past few years, as well as to outline some of the exciting opportunities for the future. This introduction is not intended to be a comprehensive review of this field and the reader is referred to detailed and excellent reviews.[7, 8, 10-12, 33, 34]

Experimental methodologies

The production of MCAs has been transformed by the advent of soft ionisation techniques and in particular electrospray ionisation (ESI).[35] In ESI, a solution containing the ion of interest is fed through a fine needle biased to a high voltage relative to the interface with a vacuum system. The ions are entrained in a flow as a fine aerosol between the ESI needle and the vacuum interface effectively closing the circuit. The polarity of the bias determines the polarity of the ion. Solvent evaporation and Coulomb explosion of the highly charged aerosol droplets ultimately leads to the formation of isolated ions. Over the past decade, the incorporation of ESI with spectroscopic techniques has flourished. The Wang group used PE spectroscopy to probe anions formed by ESI[20] and this has led to much of our core understanding of the RCB in MCAs. More recently, variations of PE spectroscopy have been combined with ESI to gain additional insight; these include PE imaging[36-41] and time-resolved PE imaging.[42-44]

PE imaging is a well-established method based on ideas taken from Houston and Chandler[45] with the important subsequent advancement of velocity-map-imaging (VMI) by Eppink and Parker.[46] In essence, any charged particle emitted onto a Newton sphere can be projected onto a position-sensitive detector, commonly formed by a pair of multi-channel plates using a phosphor screen as the anode. Charged particles impacting onto the detector are amplified through micro-channels and the localised luminescence of the phosphor is then captured using a camera. As the position sensitive detector produces a 2-dimensional image, reconstruction techniques must be used to recover the full 3D Newton sphere. This is greatly aided when there exists an axis of symmetry which is commonly imposed by the polarisation of the laser field.[47] VMI uses an electrostatic lens to image the velocity vectors of the charged particle onto a given point on the detector over a large interaction volume.[46] Although it has a near unit detection efficiency, the requirement of reconstruction algorithms necessitates high signal levels and the overall efficiency of VMI in terms of generating PE spectra is inferior to magnetic bottle type spectrometers. Magnetic bottles however cannot yield angular information and have a very poor efficiency at very low *eKE*. The additional information provided by the angularly resolved PE emission is very useful in understanding the shape of the RCB as described below. For a single photon PE image, the angular distribution is commonly described by[48, 49]

$$I(\theta) = \sigma / 4\pi \, (1 + \beta_2 P_2(\cos\theta)), \quad (3)$$

where $P_2(\cos\theta)$ is the second order Legendre polynomial, σ is the total photodetachment cross section, and β_2 is a measure of the PE anisotropy, ranging from $\beta_2 = -1$ for a perfectly perpendicular emission to $\beta_2 = +2$ for a parallel emission, relative to the laser polarisation axis.

In addition to spectral and angular resolved PE spectra, temporal resolution can be introduced using standard pump-probe methods in which a femtosecond laser pulse excites an excited state of the MCA, $[A^{n-}]^*$, and a time-delayed femtosecond probe detaches the electron from this transient excited state so that the PE spectrum corresponds to that of $[A^{n-}]^*$ at a given point along its relaxation coordinate. Time-resolved (TR) PE spectroscopy has been instrumental in understanding excited state processes in gas-phase molecules and clusters and is particularly powerful in anions as the detachment energies are often sufficiently low to enable the monitoring of the entire reaction coordinate including the ground state of the anion or MCA.[50-53] The first TR PE spectroscopy experiments on MCAs were performed by the Kappes group[30, 54] and the first direct observation of an excited state decay by electron tunnelling through the RCB was on the phthalocyanine-tetrasulfonate tetra-anion, $H_2PcSO_3^{4-}$, following *Q*-band excitation.[30] The excited state lifetime was measured to be ~70 ps. More recently, our group has developed a TR PE imaging instrument coupled to an ESI source[42, 55] to study the dynamics of MCAs providing energetic, angular and temporal resolution.

Other important recent experimental developments include the incorporation of an ion mobility cell prior to PE spectroscopy, as demonstrated by the Kappes group.[27, 56, 57] Selection of molecular shape based on a drift time can be achieved, which enables the PE spectroscopy of isomer selected MCAs. This is a key development as ever larger molecular systems are being studied for which there are several structural isomers that are populated.[26, 27]

Although the focus in this Perspective is on PE spectroscopy, action spectroscopy of excited states of MCA can also provide insight into the RCB and into the various decay pathways that are open upon resonant excitation.[25, 26, 58-65]

Photoelectron spectroscopy via excited states as a probe for the Coulomb barrier

Excited electronic states that lie between the asymptotic energy of $A^{(n-1)-} + e^-$ and the RCB are metastable with respect to electron loss and can detach by tunnelling through the RCB. The *eKE* of such electrons produced by quantum tunnelling will be below the low energy cut-off of the PE spectrum. Their formation is not instantaneous and this can have dramatic consequences on the observed electron spectrum.

For an electronic excited state to be considered a useful probe of the RCB, several properties of the excited state need to be taken into account. Optically bright excited states offer obvious experimental benefits. The lifetime of the excited state should

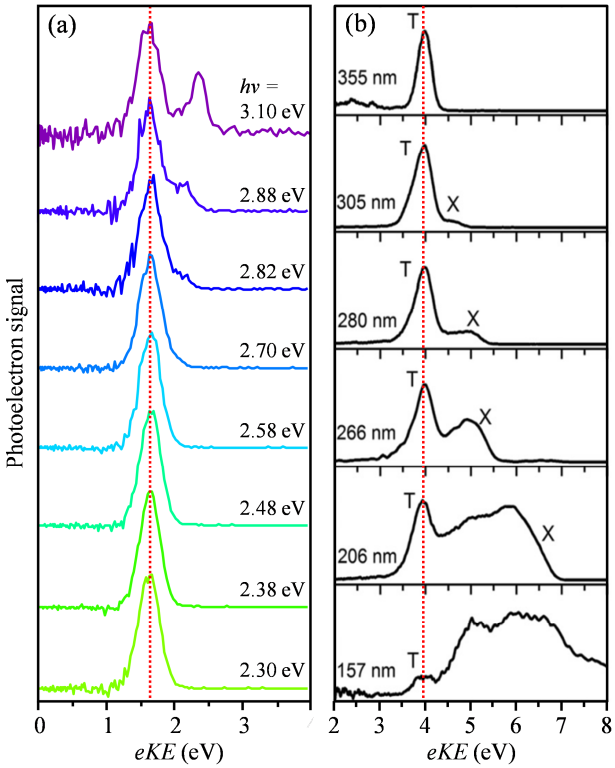

Figure 4: Photoelectron spectra of the fluorescein dianion (a) and of the bisdisulizole tetra-anion (b) taken at a range of different excitation energies. The dashed red line indicates the location of a photoelectron peak that does not shift as a function of photon energy. Adapted from Ref. 66 and 41, with permission from American Physical Society.

ideally be longer than the electron tunnelling dynamics. Internal conversion or intersystem crossing can otherwise compete with tunnelling such that the kinetics of the process is dictated by competing pathways which can mask the tunnelling dynamics. This can be achieved if the excited state lies in close proximity to the top of the RCB such that the tunnelling dynamics are fast. Alternatively, a MCA with long excited state lifetimes can be used. Fluorophores lend themselves very well to the above requirements, with strong $S_1 \leftarrow S_0$ transitions and excited state lifetimes of nanoseconds (in solution). The lowest lying spin-allowed excited state also avoids the problem that high-lying states can tunnel to different asymptotic detachment channels with different RCBs.

A useful system that meets all of the above requirements is the fluorescein dianion (deprotonated on the xanthene and carboxylic acid groups), Fl^{2-}. The 0-0 transition of the excited state of Fl^{2-} lies at 2.52 eV (492 nm) in solution, which is close to the top of the RCB. The PE spectra taken at several different photon energies, resonant with the S_1 state are shown in Figure 4(a).[66] These show a narrow feature centred at *eKE* = 1.64 eV for all photon energies studied. At photon energies higher than 2.6 eV, an additional feature can be seen and this shifts towards higher *eKE* by an amount equal to the photon energy increase; as is normally observed in direct PE spectroscopy. In contrast, the feature at 1.64 eV suggests that the electron binding energy is increasing linearly with increasing photon energy. Naturally, the *ADE* cannot change and therefore the observation points to an increase in the internal energy of the asymptotic products. At

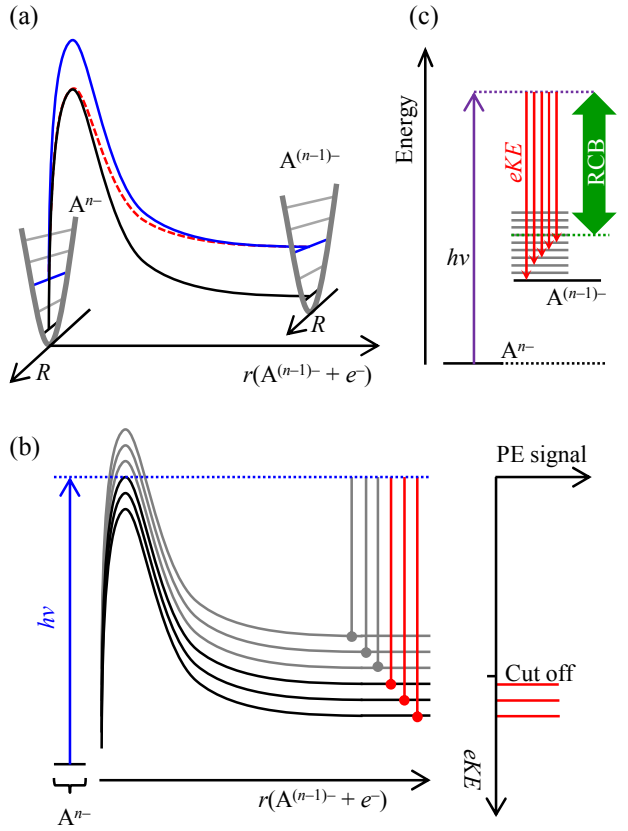

Figure 5: Energy level diagrams including the repulsive Coulomb barrier (RCB). (a) Schematic indicating a constant inner RCB (dashed red) or constant outer RCB (solid blue) as a function of internal energy. The intramolecular potential is depicted as a function of the internal coordinates, *R* of A^{n-} and $A^{(n-1)-}$. (b) Energy level diagram showing a vibronic progression of RCBs and the origin of the cut-off in the photoelectron spectrum of a MCA for direct detachment. (c) A Jablonski-type diagram incorporating the RCB.

higher photon energy, higher vibrational levels of the S_1 state are accessed so that the initial internal energy content is also larger. Rapid electron loss by tunnelling conserves this energy. Hence, for each vibrational energy level of the asymptotic products, there exists an RCB surface that connects to the same modes in the dianion. If tunnelling is fast, then there will be relatively little internal vibration redistribution and the tunnelling is adiabatic. Consequently, the transition appears as a diagonal transition. Similar features have also been seen in the PE spectroscopy of monoanions when the photon is resonant with a transition above threshold.[67]

One can imagine two limiting physical pictures to describe the observations (Figure 5(a)). The RCB viewed from the perspective of A^{n-} (the inner RCB) remains constant, while the RCB viewed from the perspective of e^- approaching $A^{(n-1)-}$ (the outer RCB) decreases; or the outer RCB remains constant and the inner RCB increases. The intramolecular potential is indicated as a function of the internal modes of A^{n-} and $A^{(n-1)-}$, which we collectively label as *R*. The intramolecular potential of course exists along the entire *r* coordinate, but has been omitted for clarity.

TR PE spectroscopy measurements on Fl^{2-} clearly support the the case in which the outer RCB remains constant (solid blue line in Figure 5(a)). Because quantum tunnelling is highly sensitive to

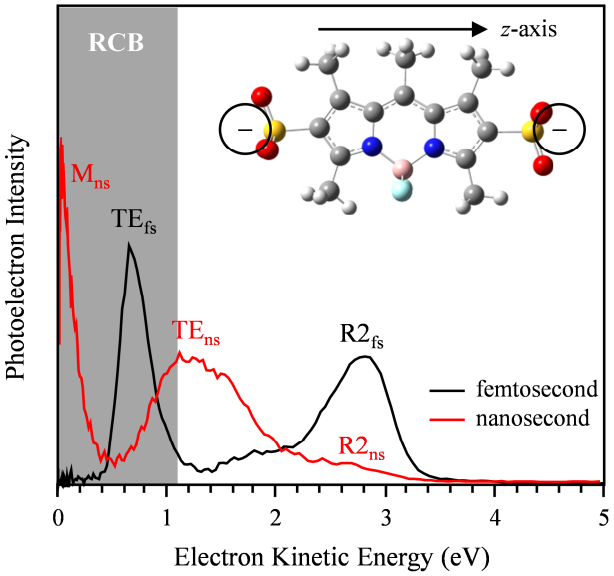

Figure 6: Photoelectron spectra of pyrromethene 556 dianion taken at 2.38 eV with a nanosecond (ns) laser and at 2.43 eV with a femtosecond (fs) laser.‡ Grey shading indicates the kinetic energy cut-off due to the RCB. Labels indicate the following: R2, two-photon resonance enhanced detachment: TE, tunnelling emission; and M, emission from the monoanion. Adapted from Ref. 44 and 68, with permission from American Chemical Society and American Institute of Physics.

the height and width of the RCB, the lifetime of the S_1 state is expected to be sensitive to changes in the internal energy content if the inner RCB remained constant. When monitoring the lifetime of the S_1, a lifetime of ~ 1 ps was observed over an excitation range of 0.3 eV, strongly pointing to a constant outer RCB.[66] This also explains why, at higher photon energies, the PE peak arising from tunnelling through the RCB (*eKE* = 1.64 eV), remains visible despite the fact that direct detachment can also occur. Even though direct detachment is an open channel (evidenced by the shifting peak in the PE spectra for $h\nu > 2.6$ eV), excitation to S_1 still occurs too and this has an associated RCB through which the electron must tunnel to access the continuum leading to an invariant *eKE*.

Similar tunnelling features at constant *eKE* have been observed by the Wang and Kappes groups in their study of a bisdisulizole tetra-anion.[41] Remarkably, this feature can be seen in the PE spectra over a photon range from $3.5 < h\nu < 7.9$ eV, as shown in Figure 4(b). It is difficult to reconcile that a single electronically excited state is involved over such a vast range. Instead, it was suggested that the initially excited state internally converts to the lowest energy state from which it would then tunnel through the RCB. This would be in-line with Kasha's rules. However, the tunnelling lifetime was also determined using TR PE spectroscopy and found to be 450 fs,[41] which suggests that the internal conversion between the excited states should be on a timescale faster than this. Similar to the case of Fl^{2-}, the short lifetime and rapid loss due to tunnelling conserves the internal energy and the tunnelling is adiabatic. Importantly, these experiments show that resonances can dramatically alter the PE spectra and, unless measurements are taken at a number of different photon energies, PE spectra can be misinterpreted.

This physical picture for the RCBs provides a clear explanation for the cut-off in PE spectra of MCAs. Perhaps the easiest way to consider the cut-off is, if one tunes $h\nu$, then no PE emission will be observed (neglecting tunnelling) until the top of the RCB is reached.[58] At this point, the energy of the emitted electron will be equal to the outer RCB height and so this is the minimum *eKE*. This picture has a problem in that several rovibrational levels or even excited electronic states can be accessed in the $A^{(n-1)-}$ product. This would lead to the emission of a PE with an *eKE* below the cut-off. From the viewpoint of the $A^{(n-1)-} + e^-$ asymptote, as the RCB is a purely electronic interaction, each vibrational energy level will have a similar RCB as shown in Figure 5(b) (note that in this figure, the intramolecular potential has been omitted for clarity). Hence, because detachment is essentially an instantaneous process, even when $h\nu >$ RCB + *ADE* only those final vibrational levels in $A^{(n-1)-}$ with energy $E_v < h\nu$ – RCB – *ADE* can be accessed. Electronically excited states in $A^{(n-1)-}$ may have different RCBs. In a Jablonski-type diagram to describe a PE experiment, the RCB should be accounted for by considering the available energy for the PE relative to $h\nu$ – RCB. An example is shown in Figure 5(c).

In cases where the tunnelling dynamics is slow and other relaxation processes may compete, the observed PE spectra can become even more difficult to interpret and can depend very sensitively on the nature of the excitation light. Figure 6 shows the PE spectra of the doubly deprotonated laser dye pyrromethene-556 dianion (PM^{2-}) taken at 2.43 eV (510 nm) with a femtosecond laser source (pulses ~100 fs duration) and at 2.38 eV (520 nm) with a nanosecond laser source‡ (pulses ~10 ns duration).[68] This photon energy is resonant with the bright $S_1 \leftarrow S_0$ transition. The peaks indicated as $R2_{fs}$ or $R2_{ns}$ arise from resonance-enhanced two-photon detachment into the continuum. The peaks indicated as TE_{fs} or TE_{ns} arise from tunnelling emission through the RCB; the RCB cut-off (determined from a PE spectrum taken at 4.66 eV) is indicated as the grey shaded region. Peaks TE_{fs} and TE_{ns}, although originating from the same process, have a dramatically different appearance. While TE_{fs} is a relatively narrow peak that does not shift in *eKE* with photon energy,[68] similar to that seen in Fl^{2-} and the bisdisulizole tetra-anion, TE_{ns} is very broad and its centre has shifted relative to TE_{fs}. Additionally, a new feature M_{ns}, peaking at *eKE* = 0 has emerged following nanosecond excitation. Qualitatively similar PE spectra were observed at a range of photon energies resonant with the $S_1 \leftarrow S_0$ transition.[68]

The differences between the PE spectra arise because the timescale of the experiments are different. Specifically, the internal conversion rate from S_1 back to S_0, which was measured to be ~120 ps,[68] exceeds the tunnelling rate and is much shorter than a nanosecond pulse but longer than a femtosecond pulse. Consequently, during the nanosecond pulse, population returns to S_0 by converting the electronic energy into vibrational energy (or heat) as the intramolecular vibration redistribution rate is also faster.[21, 24, 68] Hence, a number of photons are cycled between the $S_1 \leftarrow S_0$ transition leading to a very high internal energy content in PM^{2-}. This eventually leads to either fragmentation or electron loss over the lowest inner RCB. Fragmentation is evidenced by the low energy peak which arises from hot electron loss from a monoanion. This was first seen and described by the Wang group following excitation of a dicarboxylic acid (see Figure 7 below).[39]

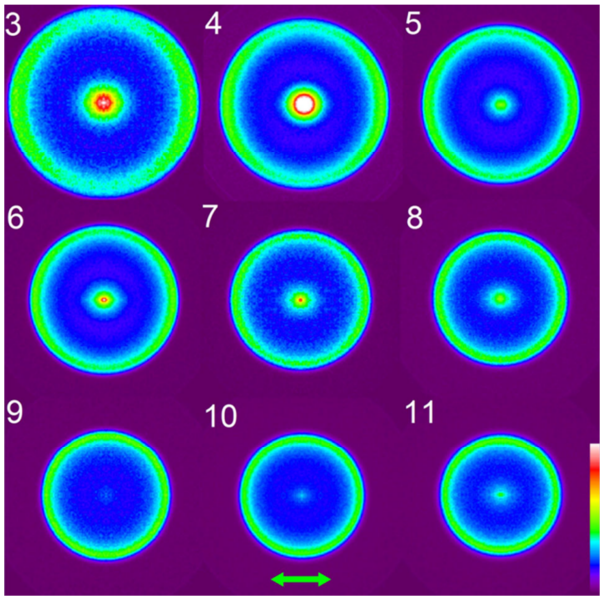

Figure 7: Photoelectron images of $^{-}O_2C(CH_2)_mCO_2^{-}$ for $3 \leq m \leq 11$ taken at 3.496 eV. The laser polarisation is indicated and is horizontal. Taken from Ref. 36 with permission from American Physical Society.

Importantly, such peaks are often not observable in magnetic bottle PE spectrometers which have very low efficiency at low *eKE*. The loss of electrons over the lowest inner RCB of the dianion leads to the observed broadening and shifting towards the RCB cut-off as seen in feature TE_{ns} in Figure 6.

The statistical detachment process differs from the adiabatic tunnelling picture as there is now sufficient time to sample those modes that lead to detachment over the lowest RCB and the physical picture becomes one in which the inner RCB appears approximately constant. In Figure 5(a), this is represented as the red dashed line. The two limiting cases in Figure 5(a) depend on the timescales of tunnelling. The idea of statistical emission over the RCB is of course important to understanding how electron detachment may arise in activated statistical dissociation processes such as collisionally induced dissociation (CID) or IR multiphoton dissociation (IRMPD).[69] These require that the inner RCB remains approximately constant because a constant outer RCB would inhibit electron loss.

The RCB has important consequences for PE spectroscopy of MCAs that should be taken into account. In particular, if a bright chromophore is present at the photon energy used, then the PE spectrum measured cannot be directly linked to the static electronic structure picture that is commonly used to explain PE features. Many biological systems fall into this category including all oligonucleotides[27, 70, 71] and many polypeptides.[25, 26, 61, 62, 64, 65] For the former, the internal conversion dynamics are extremely fast[72] and PE emission below the cut-off is a strong indicator of excited state processes and multiple-photon absorption. For the aromatic amino acids, the excited states are generally fluorescent and tunnelling through the RCB may be expected to be faster than ground state recovery.

Photoelectron angular distributions as a measure of molecular shape

Photoelectron imaging provides an additional dimension that is

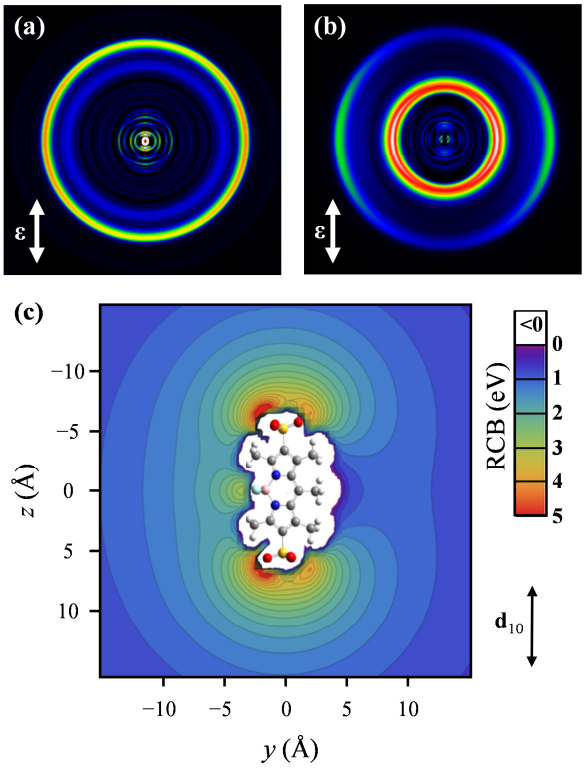

Figure 8: Photoelectron imaging of pyrromethene 556 dianions taken at (a) 4.66 eV and (b) 2.43 eV, where the latter energy is resonant with the $S_1 \leftarrow S_0$ transition. (c) The calculated RCB in the plane of the molecule, where $\mathbf{d_{10}}$ indicates the direction of the transition dipole moment. The laser polarisations are indicated in (a) and (b). Adapted from Ref. 44 and 68, with permission from American Chemical Society and American Institute of Physics.

particularly useful for MCAs. The RCB is highly anisotropic with maxima centred at localised charge sites. Classically then, an electron ejected from such a system would experience the anisotropic RCB providing a directional force onto the outgoing electron, that can ultimately "guide" the photoelectron in a specific direction. Such directional emission can, in principle, be observed through PE imaging.

The first PE imaging was performed by the Wang group on dicarboxylic acid $^{-}O_2C(CH_2)_mCO_2^{-}$ dianions at 3.496 eV.[36] Their results are shown in Figure 7 for a $3 \leq m \leq 11$ and were interpreted as follows. The photon used is sufficient to directly remove an electron from one of the carboxylic acid groups. The charge on the opposite side of the molecule remains and produces a large RCB localised on this CO_2 group. As a result, the outgoing electron experiences a repulsive force driving the electron in a direction that avoids this barrier. They also showed that the natural PE anisotropy for a carboxylic acid group (i.e. $m \rightarrow \infty$) is in the direction perpendicular to the polarisation axis which accounts for the slightly negative PE anisotropy observed for $m = 11$.[36] At higher photon energy (4.661 eV), the anisotropy reflects more that of the isolated carboxylic acid group as the RCB has a weaker effect on the much more energetic photodetached electron.[37]

However, the above experiments rely on an anisotropy in the differential cross-section to photodetachment as the sample is randomly aligned in the molecular frame. Without an *a priori*

knowledge of the differential photodetachment cross section, it is difficult to interpret the results from direct photodetachment. As an example, in Figure 8(a), the PE image of PM^{2-} is shown at 4.66 eV, which is almost isotropic despite the well-localised charges on the SO_3^- groups. Additionally, the PE angular distribution from monoanion photodetachment is governed by the interference of the outgoing partial waves and requires knowledge of the phase and cross-section into each channel.[73, 74] Hence, a direct comparison between the dianion and anion must be done with great care. An alternative method was developed in our group which employs a well-defined transition to align (in one dimension) an MCA before detachment.[44] The transition dipole moment can be readily calculated using *ab initio* methods. Resonant excitation with a polarised laser field will selectively induce a transition of the chromophore in the MCA leading to an aligned ensemble of excited MCAs, distributed as $\cos^2\theta$, where θ is the angle between the transition moment and the polarisation vectors. The photodetachment from this ensemble of electronically excited MCAs will then experience a RCB, which is now fixed in the laboratory frame as measured on the detector.

Using PM^{2-} as a representative example, the $S_1 \leftarrow S_0$ transition, which is centred around 2.4 eV has its transition dipole moment aligned along the central chromophore (*z*-axis in Figure 6).[44] Figure 8(b) shows the PE image following irradiation of PM^{2-} with 100 fs laser pulses at 2.43 eV (510 nm) along with a PE image taken at 4.66 eV. The 4.66 eV photon is above the RCB + *ADE* and so corresponds to a single-photon detachment process. In contrast, 2-photons at 2.43 eV are required. The first is resonant with the $S_1 \leftarrow S_0$ transition and produces an aligned distribution of excited state PM^{2-}. From this ensemble the second photon detaches the electron, during the 100 fs pulse. The result is a strongly peaked PE angular distribution in the direction perpendicular to the transition moment (alignment axis). The qualitative interpretation is now straight forward. In Figure 8(c), the calculated RCB in the plane of the molecule is also shown in which the transition dipole moment axis is indicated. The PE will be emitted from the central chromophore and will avoid the large peaks in the RCB near the SO_3^- groups. Hence, the observed PE distribution will peak in a direction perpendicular to the polarisation axis as observed experimentally. The same correlation between transition dipole moment, location of charged sites and PE angular distribution has been observed in the resonance-enhanced 2-photon detachment of a number of systems with different chromophores including indigo carmine[24] and a number of azobenzene derivatives.[75]

The interpretation presented here is purely qualitatively and based on classical arguments of an electron "rolling" on the RCB. However naïve this picture may be because electrons are quantum particles, it appears to capture the physics remarkably well. Quantum mechanically, a PE wave is composed of partial waves which interfere to produce the asymptotic PE angular distribution commonly observed in anions or neutrals.[73] In MCAs, it appears that this inherent anisotropy is trumped by the influence of the RCB and classical mechanics dominates. That is not to say that all interference is lost and we anticipate that, under the right conditions, quantum effects should be observable. Nevertheless, a simple molecular dynamics simulation of electron trajectories on a calculated RCB and sampled over a $\cos^2\theta$

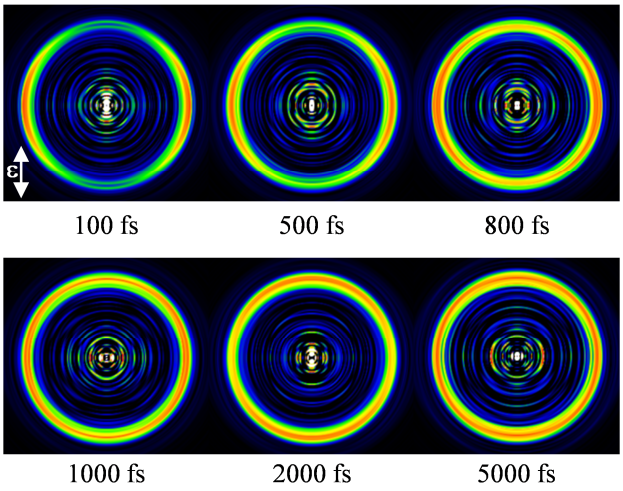

Figure 9: Time-resolved photoelectron images following excitation of pyrromethene 556 dianions to their S_1 excited state with a 2.43 eV pump and probed at 1.55 eV. The parallel laser polarisations are indicated and are vertical. Taken from Ref. 44 with permission from American Chemical Society.

distribution recovers the experimentally observed PE remarkably well. To make a full quantitative comparison would require knowledge of the differential photodetachment cross section from the excited state, which can be measured using different relative polarisations of the pump and probe fields.

An interesting consequence of this classical picture is that it allows crude structural information to be gleaned from the PE angular distribution. Specifically, the structure and charge localisation determines the RCB, which in turn determines the PE angular distribution. Hence, the two are inherently linked and the PE angular distribution can be interpreted as a crude measure of where charges are localised in the molecular framework of the MCA.[44] Indeed, it suggests that one can track the temporal evolution (molecular dynamics) of a MCA by monitoring the PE angular distribution.

Using PM^{2-} as an example again, Figure 8(b) also shows an additional feature at lower energy (smaller radius) which can be correlated with the tunnelling through the RCB as the adiabatic energy (1.6 eV) lies below the S_1 state but the RCB above it. This PE feature is almost isotropic because the timescale for electron emission is slower than the rotational dephasing time of the system. Hence, on the timescale of electron emission, the alignment and correlation between laboratory and molecular frames of reference is lost. These molecular dynamics can be monitored in real-time in a pump probe TR PE imaging experiment.[44] Figure 9 shows the PE images as a function of delay between a 2.43 eV pump and 1.55 eV probe (parallel polarisation) with an overall temporal resolution of ~100 fs. At very early times, the PE emission is peaked in a direction perpendicular to the polarisation of the laser fields, as described above. However, as time evolves, the anisotropy decreases and even becomes slightly positive at $t \sim 2$ ps (i.e. aligned along the polarisation axes), before settling around $\beta_2 = 0$. The anisotropy can be correlated with the laboratory frame alignment. At early times, the S_1 excited ensemble is aligned parallel to the polarisation axes, leading to perpendicular emission because of the RCB. At ~2 ps, the rotational coherence has evolved and on

average, the ensemble has undergone a $\pi/2$ rotation so that the ensemble is aligned perpendicular to the polarisation axes and the RCB guides the electrons in a direction parallel to the polarisation axes. At longer times, the wavepacket is fully dephased and the ensemble appears as an isotropic distribution.

Future prospects

The discussion in the preceding section highlights that molecular dynamics can be monitored in real-time through TR PE imaging of MCAs. Taking this forward, large-amplitude structural dynamics could also be observable in real-time. For example, photo-induced isomerisation or ring-opening reactions could be monitored if either end of the chromophore has a localised charged group such as CO_2^- or SO_3^-. Following excitation, the PE angular distributions would differ significantly because the relative positions of the charged groups would change and hence the RCB becomes a time-dependent property of the MCA. In addition to changes in PE angular distributions, the distance between charged groups will be affected such that the cut-off in the PE spectrum will also change (proportional to R^{-1}) as a function of time.

The above would require direct comparison with calculated PE images based on time-dependent structures (and corresponding RCB) along the reaction coordinate. At present, no quantitative comparisons have been made between experimentally observed PE images and simulated ones. Classically, the simulation would be quite straight-forward, however, whether quantum effects can be ignored remains an open question. Quantum effects may in fact turn out to be highly informative and one can envisage interference patterns akin to electron diffraction patterns following photodetachment. No evidence of interference has yet been observed in the PE angular distributions, although this is likely a consequence of the relatively high temperatures of the MCAs. Specifically, most experiments thermalize the MCA in a room temperature trap such that the ions have a 300 K internal energy distribution. Recently, cryogenic ion traps have been incorporated and these can bring the ions down to ~10 K at which point much of the thermal fluctuations are removed. In terms of alignment experiments as described above, such low temperatures would also lead to much slower rotational dynamics. Moreover, the RCB cut-off measured experimentally is likely to be sensitive to temperature and is expected to be much more well-defined at low T.

Thus far, alignment has only been imposed by a resonant excitation with a maximum alignment of $\cos^2\theta$. This distribution is also transferred onto the PE angular distribution smearing the molecular frame anisotropy and potentially masking quantum effects. Higher degrees of alignment are possible using appropriate (strong) laser fields.[76, 77] The degree of alignment in such experiments depends on the polarisation anisotropy of the molecular system and this can be very large for MCAs. However, the strong laser fields also affect the RCB. Specifically, the strong electric fields required alter the RCB such that, even at relatively low laser intensities, tunnel ionisation becomes important. This can be clearly seen in PE spectra as now electrons can be emitted with *eKE* below the cut-off.[24]

It is also worth considering the final state produced by photodetachment from excited states. As the excited states are often those of a *neutral* chromophore within the MCA, photodetachment from excited states results in a zwitter-ionic anion or MCA: both localised positive and negative are present although the overall charge remains negative. This can also be done in anions leading to zwitter-ionic neutrals.[78, 79] These final states are not necessarily the ground electronic state but require the migration of charge and electron-hole recombination to decay. Such processes can be difficult to study in real time in the gas phase. MCAs offer an elegant route to studying these processes in which a pump pulse remove the electron leaving an excited state zwitter-ion, the decay of which can be monitored using TR PE spectroscopy.

Finally, MCAs presents opportunities to probe solvation on a molecular level such as hydrophobic and hydrophilic interactions and the balance between charge-repulsion, solvation and hydrogen bonding.[80-84] Excited states provide a route to understanding solvation dynamics in real-time and how solvent responds to, for example, charge-injection or removal[4, 85-87] or solvent caging effects following dissociation.[88, 89] The fact that more than one negative charge is present in an MCA poses several interesting questions. For example, how much solvent is required to cage a Coulomb explosion or to solvate an electron following charge-transfer to solvent from an MCA? TR PE spectroscopy is ideally suited to monitor these types of processes as it is not limited to a spectral window and can monitor the entire reaction coordinate.

Acknowledgment

This work has been supported by the EPSRC (EP/D073472/1) and the ERC through a Starting Grant (306536).

Notes and references

‡ In reference 68, a PE spectrum is also provided at (2.38 eV) 520 nm with a femtosecond laser to match the photon energy of the ns PE spectrum. This is essentially the same as the PE spectrum at 2.43 eV with a shift of 0.10 eV in the R2fs peak. The 2.43 eV fs PE spectrum was used for its higher signal to noise.

[a] *Department of Chemistry, University of Durham, Durham DH1 3LE, United Kingdom.*
[b] *Center for Free-Electron Laser Science, DESY, Notkestraße 85, 22607 Hamburg, Germany.*
[c], *Ultrafast X-ray Science Laboratory,1 Cyclotron Road, Berkeley CA 94720, USA.*
* *Correspondence: j.r.r.verlet@durham.ac.uk*

1. A. I. Boldyrev and J. Simons, *Journal of Physical Chemistry*, 1994, **98**, 2298.
2. X. B. Wang, J. B. Nicholas and L. S. Wang, *Journal of Physical Chemistry A*, 2000, **104**, 504.
3. X. B. Wang, J. B. Nicholas and L. S. Wang, *Journal of Chemical Physics*, 2000, **113**, 10837.
4. X. B. Wang, X. Yang, J. B. Nicholas and L. S. Wang, *Science*, 2001, **294**, 1322.
5. A. Whitehead, R. Barrios and J. Simons, *Journal of Chemical Physics*, 2002, **116**, 2848.
6. X. Yang, X. B. Wang and L. S. Wang, *Journal of Physical Chemistry A*, 2002, **106**, 7607.
7. M. K. Scheller, R. N. Compton and L. S. Cederbaum, *Science*, 1995, **270**, 1160.
8. A. I. Boldyrev, M. Gutowski and J. Simons, *Accounts of Chemical Research*, 1996, **29**, 497.
9. C. F. Ding, X. B. Wang and L. S. Wang, *Journal of Physical Chemistry A*, 1998, **102**, 8633.

10. A. Dreuw and L. S. Cederbaum, *Chemical Reviews*, 2002, **102**, 181.
11. X. B. Wang, X. Yang and L. S. Wang, *International Reviews in Physical Chemistry*, 2002, **21**, 473.
12. X.-B. Wang and L.-S. Wang, in *Annual Review of Physical Chemistry*, 2009, **60**, 105.
13. T. F. Omalley, *Phys. Rev.*, 1965, **137**, 1668.
14. S. N. Schauer, P. Williams and R. N. Compton, *Physical Review Letters*, 1990, **65**, 625.
15. R. L. Hettich, R. N. Compton and R. H. Ritchie, *Physical Review Letters*, 1991, **67**, 1242.
16. P. A. Limbach, L. Schweikhard, K. A. Cowen, M. T. McDermott, A. G. Marshall and J. V. Coe, *Journal of the American Chemical Society*, 1991, **113**, 6795.
17. T. Sommerfeld, M. K. Scheller and L. S. Cederbaum, *Chemical Physics Letters*, 1993, **209**, 216.
18. L. S. Wang, C. F. Ding, X. B. Wang, J. B. Nicholas and B. Nicholas, *Physical Review Letters*, 1998, **81**, 2667.
19. X. B. Wang, C. F. Ding and L. S. Wang, *Physical Review Letters*, 1998, **81**, 3351.
20. L. S. Wang, C. F. Ding, X. B. Wang and S. E. Barlow, *Review of Scientific Instruments*, 1999, **70**, 1957.
21. A. S. Chatterley, D. A. Horke and J. R. R. Verlet, *Physical Chemistry Chemical Physics*, 2012, **14**, 16155.
22. O. T. Ehrler, J. M. Weber, F. Furche and M. M. Kappes, *Physical Review Letters*, 2003, **91**, 113006.
23. O. T. Ehrler, F. Furche, J. M. Weber and M. M. Kappes, *Journal of Chemical Physics*, 2005, **122**, 094321.
24. A. S. Chatterley, D. A. Horke and J. R. R. Verlet, *Physical Chemistry Chemical Physics*, 2014, **16**, 489.
25. K. Matheis, L. Joly, R. Antoine, F. Lepine, C. Bordas, O. T. Ehrler, A.-R. Allouche, M. M. Kappes and P. Dugourd, *Journal of the American Chemical Society*, 2008, **130**, 15903.
26. M. Vonderach, O. T. Ehrler, K. Matheis, T. Karpuschkin, E. Papalazarou, C. Brunet, R. Antoine, P. Weis, O. Hampe, M. M. Kappes and P. Dugourd, *Physical Chemistry Chemical Physics*, 2011, **13**, 15554.
27. M. Vonderach, O. T. Ehrler, K. Matheis, P. Weis and M. M. Kappes, *Journal of the American Chemical Society*, 2012, **134**, 7830.
28. X. B. Wang and L. S. Wang, *Nature*, 1999, **400**, 245.
29. K. Arnold, T. S. Balaban, M. N. Blom, O. T. Ehrler, S. Gilb, O. Hampe, J. E. van Lier, J. M. Weber and M. M. Kappes, *Journal of Physical Chemistry A*, 2003, **107**, 794.
30. O. T. Ehrler, J.-P. Yang, A. B. Sugiharto, A. N. Unterreiner and M. M. Kappes, *Journal of Chemical Physics*, 2007, **127**, 80842.
31. J. Yang, X.-P. Xing, X.-B. Wang, L.-S. Wang, A. P. Sergeeva and A. I. Boldyrev, *Journal of Chemical Physics*, 2008, **128**, 091102.
32. A. Dreuw and L. S. Cederbaum, *Physical Review A*, 2001, **63**, 049904.
33. L. S. Wang and X. B. Wang, *Journal of Physical Chemistry A*, 2000, **104**, 1978.
34. J. Simons, *Journal of Physical Chemistry A*, 2008, **112**, 6401.
35. J. B. Fenn, M. Mann, C. K. Meng, S. F. Wong and C. M. Whitehouse, *Science*, 1989, **246**, 64.
36. X.-P. Xing, X.-B. Wang and L.-S. Wang, *Physical Review Letters*, 2008, **101**, 083003.
37. X.-P. Xing, X.-B. Wang and L.-S. Wang, *Journal of Chemical Physics*, 2009, **130**, 074301.
38. X.-P. Xing, X.-B. Wang and L.-S. Wang, *Journal of Physical Chemistry A*, 2009, **113**, 945.
39. X.-P. Xing, X.-B. Wang and L.-S. Wang, *Journal of Physical Chemistry A*, 2010, **114**, 4524.
40. E. Papalazarou, C. Cauchy, T. Barillot, B. Bellina, J. Maurelli, M. Barbaire, C. Clavier, F. Bertorelle, R. Antoine, I. Compagnon, A. R. Allouche, C. Bordas, P. Dugourd and F. Lepine, *Analyst*, 2012, **137**, 3496.
41. D. Phuong Diem, H.-T. Liu, J.-P. Yang, M.-O. Winghart, T. J. A. Wolf, A.-N. Unterreiner, P. Weis, Y.-R. Miao, C.-G. Ning, M. M. Kappes and L.-S. Wang, *Physical Review A*, 2012, **85**, 064503.
42. J. Lecointre, G. M. Roberts, D. A. Horke and J. R. R. Verlet, *Journal of Physical Chemistry A*, 2010, **114**, 11216.
43. D. A. Horke and J. R. R. Verlet, *Physical Chemistry Chemical Physics*, 2011, **13**, 19546.
44. D. A. Horke, A. S. Chatterley and J. R. R. Verlet, *Journal of Physical Chemistry Letters*, 2012, **3**, 834.
45. D. W. Chandler and P. L. Houston, *Journal of Chemical Physics*, 1987, **87**, 1445.
46. A. Eppink and D. H. Parker, *Review of Scientific Instruments*, 1997, **68**, 3477.
47. *Imaging in Molecular Dynamics*, Cambridge University Press, 2007.
48. K. L. Reid, *Annual Review of Physical Chemistry*, 2003, **54**, 397.
49. K. L. Reid, *Molecular Physics*, 2012, **110**, 131.
50. A. Stolow, A. E. Bragg and D. M. Neumark, *Chemical Reviews*, 2004, **104**, 1719.
51. T. Suzuki, in *Annual Review of Physical Chemistry*, 2006, **57**, 555.
52. T. Suzuki, *International Reviews in Physical Chemistry*, 2012, **31**, 265.
53. J. R. R. Verlet, *Chemical Society Reviews*, 2008, **37**, 505.
54. C. Rensing, O. T. Ehrler, J.-P. Yang, A.-N. Unterreiner and M. M. Kappes, *Journal of Chemical Physics*, 2009, **130**, 234306.
55. D. A. Horke, G. M. Roberts, J. Lecointre and J. R. R. Verlet, *Review of Scientific Instruments*, 2012, **83**, 053104.
56. M. Vonderach, O. T. Ehrler, P. Weis and M. M. Kappes, *Analytical Chemistry*, 2011, **83**, 1108.
57. K. Matheis, A. Eichhoefer, F. Weigend, O. T. Ehrler, O. Hampe and M. M. Kappes, *Journal of Physical Chemistry C*, 2012, **116**, 13800.
58. D. Loffler, J. M. Weber and M. M. Kappes, *Journal of Chemical Physics*, 2005, **123**, 224308.
59. J. C. Marcum and J. M. Weber, *Journal of Chemical Physics*, 2009, **131**, 194309.
60. S. H. Kaufman, J. M. Weber and M. Pernpointner, *Journal of Chemical Physics*, 2013, **139**, 194310.
61. L. Joly, R. Antoine, A.-R. Allouche, M. Broyer, J. Lemoine and P. Dugourd, *Journal of the American Chemical Society*, 2007, **129**, 8428.
62. L. Joly, R. Antoine, M. Broyer, J. Lemoine and P. Dugourd, *Journal of Physical Chemistry A*, 2008, **112**, 898.
63. R. Antoine and P. Dugourd, *Physical Chemistry Chemical Physics*, 2011, **13**, 16494.
64. C. Brunet, R. Antoine, P. Dugourd, F. Canon, A. Giuliani and L. Nahon, *Journal of Chemical Physics*, 2013, **138**, 064301.
65. M. Vonderach, M.-O. Winghart, L. MacAleese, F. Chirot, R. Antoine, P. Dugourd, P. Weis, O. Hampe and M. M. Kappes, *Physical Chemistry Chemical Physics*, 2014, **16**, 3007.
66. D. A. Horke, A. S. Chatterley and J. R. R. Verlet, *Physical Review Letters*, 2012, **108**, 093003.
67. D. A. Horke, Q. Li, L. Blancafort and J. R. R. Verlet, *Nature Chemistry*, 2013, **5**, 711.
68. D. A. Horke, A. S. Chatterley and J. R. R. Verlet, *Journal of Chemical Physics*, 2013, **139**, 084302.
69. S. Ard, N. Mirsaleh-Kohan, J. D. Steill, J. Oomens, S. B. Nielsen and R. N. Compton, *Journal of Chemical Physics*, 2010, **132**, 094301.
70. V. Gabelica, T. Tabarin, R. Antoine, F. Rosu, I. Compagnon, M. Broyer, E. De Pauw and P. Dugourd, *Analytical Chemistry*, 2006, **78**, 6564.
71. V. Gabelica, F. Rosu, T. Tabarin, C. Kinet, R. Antoine, M. Broyer, E. De Pauw and P. Dugourd, *Journal of the American Chemical Society*, 2007, **129**, 4706.
72. A. S. Chatterley, C. W. West, G. M. Roberts, V. G. Stavros and J. R. R. verlet, *Journal of Physical Chemistry Letters*, 2014, **5**, 843.
73. K. L. Reid, *International Reviews in Physical Chemistry*, 2008, **27**, 607.
74. A. Sanov and R. Mabbs, *International Reviews in Physical Chemistry*, 2008, **27**, 53.
75. N. P. L. Andrews, D. A. Horke, A. S. Chatterley and J. R. R. Verlet, Unpublished results show qualitativly similar PE images for sunset yellow and acid yellow 9 dianions in which the transition dipole moment was aligned along the N=N bond.
76. H. Stapelfeldt and T. Seideman, *Reviews of Modern Physics*, 2003, **75**, 543.

77. L. Holmegaard, J. L. Hansen, L. Kalhoj, S. L. Kragh, H. Stapelfeldt, F. Filsinger, J. Küpper, G. Meijer, D. Dimitrovski, M. Abu-samha, C. P. J. Martiny and L. B. Madsen, *Nature Physics*, 2010, **6**, 428.
78. X. B. Wang, J. B. Nicholas and L. S. Wang, *Journal of Chemical Physics*, 2000, **113**, 653.
79. A. S. Chatterley, A. S. Johns, V. G. Stavros and J. R. R. Verlet, *Journal of Physical Chemistry A*, 2013, **117**, 5299.
80. D. J. Goebbert, T. Wende, R. Bergmann, G. Meijer and K. R. Asmis, *Journal of Physical Chemistry A*, 2009, **113**, 5874.
81. B. Minofar, M. Mucha, P. Jungwirth, X. Yang, Y. J. Fu, X. B. Wang and L. S. Wang, *Journal of the American Chemical Society*, 2004, **126**, 11691.
82. X.-B. Wang, J. Yang and L.-S. Wang, *Journal of Physical Chemistry A*, 2008, **112**, 172.
83. M. Wanko, T. Wende, M. Montes Saralegui, L. Jiang, A. Rubio and K. R. Asmis, *Physical Chemistry Chemical Physics*, 2013, **15**, 20463.
84. X. Yang, Y. J. Fu, X. B. Wang, P. Slavicek, M. Mucha, P. Jungwirth and L. S. Wang, *Journal of the American Chemical Society*, 2004, **126**, 876.
85. A. Kammrath, G. B. Griffin, J. R. R. Verlet, R. M. Young and D. M. Neumark, *Journal of Chemical Physics*, 2007, **126**, 244306.
86. A. Kammrath, J. R. R. Verlet, A. E. Bragg, G. B. Griffin and D. M. Neumark, *Journal of Physical Chemistry A*, 2005, **109**, 11475.
87. J. R. R. Verlet, A. Kammrath, G. B. Griffin and D. M. Neumark, *Journal of Chemical Physics*, 2005, **123**, 231102.
88. B. J. Greenblatt, M. T. Zanni and D. M. Neumark, *Science*, 1997, **276**, 1675.
89. L. Sheps, E. M. Miller, S. Horvath, M. A. Thompson, R. Parson, A. B. McCoy and W. C. Lineberger, *Science*, 2010, **328**, 220.